Appl. Phys. B 39, 65–72 (1986)

Applied Physics B Photophysics and Laser Chemistry

Molecular Enhanced Four-Wave Parametric Generation in Sodium Atom

S. G. Dinev, I. G. Koprinkov*, and I. L. Stefanov

Department of Physics, Sofia University, BG-1126 Sofia, Bulgaria

Received 13 February 1985/Accepted 16 June 1985

Abstract. A number of resonances have been observed in the excitation spectrum of the uv resonance lines of sodium. The mechanism proposed includes absorption by molecular states, energy transfer to excited atomic levels and four-wave parametric generation enhanced by radiative decay of the excited states.

PACS: 42.60, 42.65

Four-wave interactions in atomic vapor have recently been studied by several authors [1–3]. Degenerate four-wave mixing enhanced by Na_A^* exciplexes via excited $3p$ state of Na has been reported by Ewart et al. [4]. Some extra resonances in the four wave mixing have been measured by foreign gas pressure induced effects [5].

In this paper we report on a number of new resonant excitation lines in the four-wave parametric interactions in sodium. The new resonance are caused by single- and two-photon transitions between molecular states. Following dissociation one of the atoms is left in an excited state or its population is transfered to another state. The resulting resonant emission to the ground state is a strong background for the signal wave ω_s in the four-wave parametric process $2\omega_d = \omega_i + \omega_s$, where ω_d is the pump laser frequency and ω_i is the idler frequency, coupled with the signal.

Very recently the work of Chen et al. [6] was published. By tuning the pump wavelength to 583.9 nm they observed the forward and orthogonal resonant fluorescence at 330 nm. The stimulated electronic Raman scattering (SERS) process proposed there as an explanation is different from the mechanism discussed in this paper.

Experimental

The dye laser used in the experiment was a home-built grazing-incidence oscillator followed by two amplification stages[1]: An excimer laser (Lambda Physik EMG 50 E) pumped the dye laser. A spatial filter and telescope in the oscillator-amplifier chain as well as a 3 ns delay line between the oscillator and amplifier pumping pulses improved the beam quality and spectral purity. The linewidth of the dye laser was $\leqq 0.1\ \mathrm{cm}^{-1}$ and the energy of the pulse was up to 1 mJ. The vapor was contained in a heat pipe with a 51 cm heated zone. The pressure of the Ar buffer gas was varied in the range 5–300 Torr. The pulse energy was controlled by an energy meter (Laser Precision Rj 7200). The pump and signal intensity was changed by calibrated neutral density glass and metalic filters, respectively (Lambda Physik Lf 304, Lf 303). The uv parametric emission was filtered, measured by a 40 cm scanning monochromator (MDR–2) and processed by a Laser photometer (Lambda Physik LM 300).

Molecular Absorption and Energy Transfer

When the dye-laser frequency was tuned to the sodium two-photon resonances $3s$–$5s$ and $3s$–$4d$, a strong

---

* Present address: Department of Physics, Higher Institute of Electrical and Mechanical Engineering, BG-1156 Sofia, Bulgaria

[1] The initial part of the measurements has been performed during the stay of one of us (S.G.D.) at the Max-Planck-Institut für Quantenoptik in Garching, FRG, using a similar dye-laser and heat-pipe system and boxcar averager

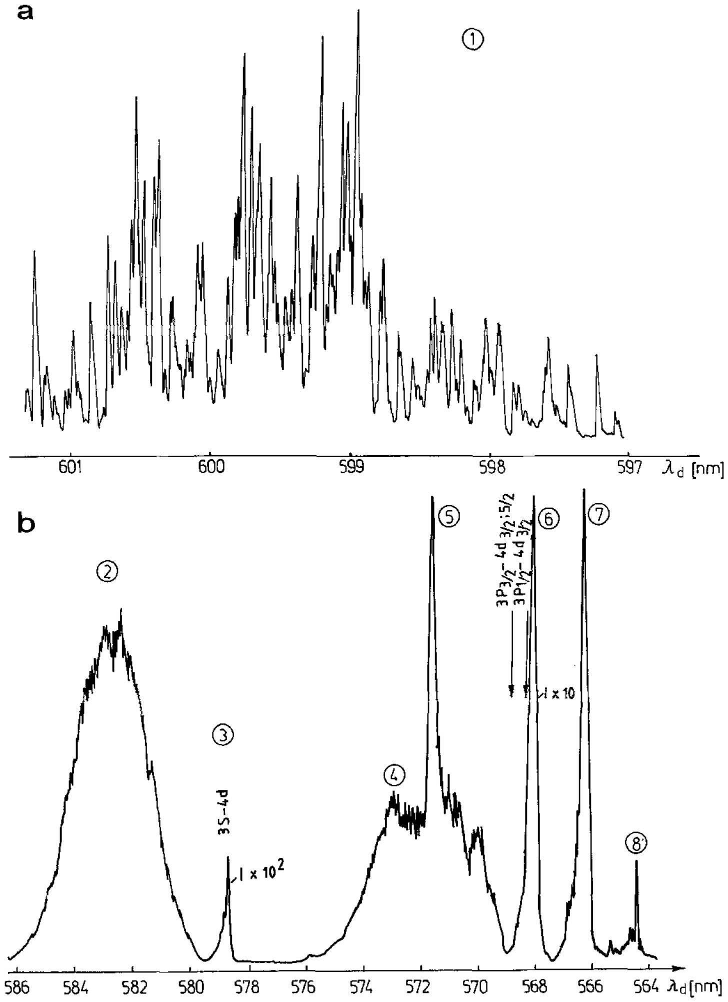

Fig. 1a and b. Excitation spectra of sodium for the generation of stimulated emission at 330 nm. (a) Dye-laser scan in the range 597–601 nm; (b) Dye-laser scan in the range 564–586 nm. The wavenumbers of the intensive lines in the spectrum marked as 1 are presented in Table 1. The line with maximum intensity in Fig. 1 corresponds to No 19 in Table 1

collimated emission at 330 nm emerged, following the well-known mechanisms [1, 3]. However, scanning the dye laser outside the atomic resonances, the 330 nm beam was excited through many narrow as well as broad resonances, which we could not identify with any atomic transition of Na. The intensity of the new lines in some cases was comparable to the atomic resonances. The strong beam was observed on a white target. The divergence measured by a diode array approximately follows the divergence of the pump laser. A part of the excitation spectrum from 597 to 601 nm is given in Fig. 1a and from 564 to 586 nm in Fig. 1b.

A potassium vapor pumped in the same wavelength region shows also a number of additional resonances, the most intense of which are 597.76, 597.71, 597,29, 597.25, 597.11, 597.05, 592.15, 591.95 and 591.22 nm. The collimated emission recorded consists of several resonant lines from high lying *n*P states of potassium atom.

The presence of complex structure in the excitation spectrum of 330 nm consisting of both discrete lines and broad bands can not be explained without taking into account the bound Na_2 dimer states and the colissional complexes Na–Ar and Na–Na. Since the parametric process discussed is in the atomic system, these states serve as a channel for energy transfer from the molecular to the atomic system. According to the mechanism proposed below this leads to enhancement of the parametric process via molecular resonances. Considering atomic levels only the intensity of the parametric light should decrease continuously by detuning from the two-photon resonances 3*s*–4*d* and 3*s*–5*s*.

Among the molecular channels leading to population of atomic levels we consider that only those contribute to the parametric process, which populate considerably and fast (within the pumping pulse) appropriate atomic levels, 4*p* in our case.

The excitation spectrum in the range 597–601 nm (Fig. 1a), consisting of a large number of discrete lines is like a single-photon bound-bound molecular spectrum. The ground state of Na_2 is $X^1\Sigma_g^+$, hence in the dipole approximation the allowed transitions are to

Table 1. Measured excitation lines ν_m, rotational and vibrational numbers v_x, J_x, v_A, J_A and difference between measured and calculated value $\Delta = \nu_m - \nu_c$ in sodium

No.	ν_m [cm^{-1}]	v_x	J_x	v_A	J_A	$\Delta = \nu_m - \nu_c$ [cm^{-1}]
1.	16744.23	0	47	20	48	−0.10
2.	16740.30	3	33	24	34	−0.29
3.	16734.14	0	49	20	50	−0.14
4.	16730.78	0	46	20	45	−0.19
5.	16724.62	2	22	22	23	−0.32
6.	16723.50	3	54	25	53	0.08
7.	16721.26	2	20	22	19	0.14
8.	16720.14	2	24	22	25	−0.13
9.	16717.91	2	25	22	26	0.12
10.	16710.92	2	24	22	23	0.25
11.	16708.97	1	43	21	44	−0.34
12.	16707.85	2	25	22	24	0.06
13.	16706.73	2	29	22	30	−0.03
14.	16703.39	0	51	20	50	−0.32
15.	16700.04	4	29	25	30	−0.11
16.	16697.25	2	32	22	33	−0.13
17.	16693.90	2	33	22	34	−0.13
18.	16692.23	0	53	20	52	0.14
19.	16691.67	2	30	22	29	−0.13
20.	16689.44	3	42	24	41	0.12
21.	16688.33	2	31	22	30	0.04
22.	16686.66	1	44	21	33	−0.07
23.	16684.43	2	32	22	31	−0.24
24.	16683.32	2	36	22	37	−0.07
25.	16679.98	2	37	22	38	0.35
26.	16674.41	1	23	20	24	−0.28
27.	16672.19	1	24	20	25	−0.13
28.	16670.52	1	21	20	20	−0.06
29.	16668.85	2	36	22	35	−0.29
30.	16667.74	1	22	20	21	−0.28
31.	16667.19	1	26	20	27	−0.07
32.	16666.09	1	48	21	48	−0.02
33.	16664.41	1	27	20	28	−0.15
34.	16661.08	0	58	20	57	−0.16
35.	16659.96	1	25	20	24	0.24
36.	16654.97	2	43	22	44	0.11
37.	16652.19	2	40	22	39	0.24
38.	16651.09	3	26	23	25	−0.39
39.	16648.87	5	25	26	24	−0.01
40.	16647.76	1	55	21	56	0.24
41.	16647.21	2	41	22	40	−0.19
42.	16643.33	1	30	20	29	−0.46
43.	16642.22	0	78	21	79	0.32
44.	16638.89	0	65	20	66	−0.18
45.	16635.57	1	36	20	37	−0.02
46.	16630.04	1	58	21	59	0.10
47.	16627.27	2	62	23	61	0.05

the $A^1\Sigma_u^+$ and $B^1\Pi_u$ states. Since $B(v'=0)$ is 20302 cm^{-1} [7] higher than $X(v''=0)$, in this spectral region $X-B$ transition can take place from ground vibrational-rotational levels 3695 cm^{-1} above the bottom, which have very low thermal population. In this way the $X-B$ transitions are excluded and the intense molecular absorption in this range is to be considered as a $X-A$ transition. For identification of the observed bound-bound excitation spectrum we have used the molecular constants for X [7] and A [8]. As an additional criterion for the assignment, the classical Franck-Condon principle was applied to the precisely tabulated curves of X and A states, given by Zemke et al. [9]. The observed frequencies, vibrational and rotational numbers of the lines, as well as the difference between measured and calculated values are given in Table 1.

The energy of one photon in the range considered is not enough to reach the dissociation limit of the excited dimer states, starting from highly populated low-lying vibrational levels of X. Therefore, the excitation lines of 330 nm are due to two-photon transitions, with a second photon in the dissociation continuum of a molecular state. According to the selection rules the second transition from the intermediate $A^1\Sigma_u^+$ state can populate $^1\Sigma_g^+$ and $^1\Pi_g$ states.

Let us consider an excitation line in the middle of the range in Fig. 1a $\nu = 16686$ cm^{-1}, taking the dissociation energy of the X state $D_e = 6024$ cm^{-1} [10].

The Na(3d) level is 35196.9 cm^{-1} [11] from the bottom of the X potential well (Fig. 2). Since $2\nu = 33372$ cm^{-1}, the dissociation continuum of the molecular states with the 3d atomic assymptote can be reached with photons starting from vibrational-

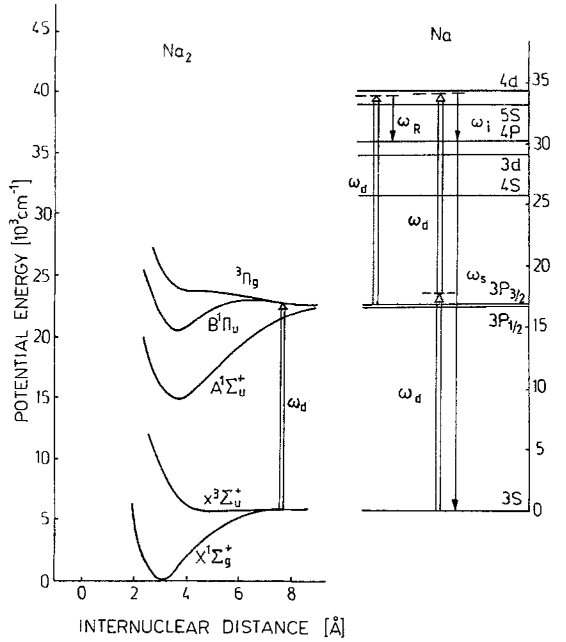

Fig. 2. Energy-level diagram of sodium as a function of internuclear separation. Shown are also transitions in the Na–Na collisional complex as well as in an Na atomic system, leading to stimulated parametric emission at 330 nm

rotational levels 1825 cm^{-1} above the bottom of X. These levels are relatively weakly populated (about 4% of all molecules at 813 K according to the Boltzman distribution) and we consider the dissociation in Na(3d) as weak. From the other side, the excitation energy 2ν is 1608 cm^{-1} above the Na(4s) level. The atomic states Na(3s) and Na(4s) lead to the formation of a singlet $^1\Sigma_g^+$ state.

$$\mathrm{Na}(4s)+\mathrm{Na}(3s)\rightarrow \mathrm{Na}_2\,{}^1\Sigma_g^+(3s+4s)\,. \tag{1}$$

Similar to $^1\Sigma_g^+$ states, obtained from $\mathrm{Na}_2(3s+3s)$, $\mathrm{Na}_2(3s+5s)$ and $\mathrm{Na}_2(3s+6s)$ (the latter two were extensively studied by Schawlow et al. [12], which are bound, we suppose that $\mathrm{Na}_2\ {}^1\Sigma_g^+(3s+4s)$ is also bound. In this way, the two-photon transition from $^1\Sigma_g^+(3s+3s)$ can terminate on the repulsive part of the $^1\Sigma_g^+(3s+4s)$ potential at small internuclear distances about 1600 cm^{-1} above the dissociation limit. This leads to population of the 4s state after dissociation. Since the second photon is in the continuum, we conclude that the excitation lines observed correspond the exact $X-A$ vibrational-rotational resonances.

The dye-laser wavelength λ_d in this region is ~300 cm^{-1} off resonance in the red wing of the atomic 3P line. Therefore, the 3P level would not be considerably populated via Na–Ar or Na–Na collisional complexes. In this way in the initial stage of the pumping-pulse conditions for laser generation in the 4s–3p ir transition can be formed. Unfortunately, this transition wavelength $\lambda(4s\text{–}3p)=1140.4$ nm is outside the detection range of the measuring system available. Infrared laser emission in K, Cs and Rb has been observed by Sorokin and Lankard [13]. In their experiment the atomic levels were populated by dissociation of two-photon excited dimers.

In our case, 4s–3p is the only channel for radiative relaxation of 4s, and a considerable fraction of the 4s population will be transfered to 3p.

Concerning the 4p level, there are several mechanisms leading to transfer of population from 3p to 4p directly or after radiative relaxation from higher-lying levels:

1) Stimulated electronic Raman scattering SERS with excited 3p as initial state and 4p as a final state.

2) Energy pooling colission of the type [14]

$$\mathrm{Na}(3p)+\mathrm{Na}(3p)\rightarrow \mathrm{Na}(nl)+\mathrm{Na}(3s) \tag{2}$$

where nl are 4d, 5s and 4p levels.

3) Associative ionization with the product Na_2^+. The dimer ion dissociates by recombination.

Let us now evaluate the time constants for the population of a particular nl state, using the energy pooling mechanism. The rate constants given in the literature differ by orders of magnitude. We have used the data given by Kushawaha et al. [15, 16]

$$k_{4\mathrm{d}}=5.10^{-15}\,\mathrm{cm}^3\,\mathrm{s}^{-1}\ \text{at}\ T=510\,K \quad [15]\,, \tag{3}$$

$$k_{5\mathrm{s}}=7.10^{-15}\,\mathrm{cm}^3\,\mathrm{s}^{-1}\text{independent of temperature}\ T \quad [15]\,, \tag{4}$$

$$k_{4\mathrm{p}}=3.10^{-16}\,\mathrm{cm}^3\,\mathrm{s}^{-1}\text{at}\ T=487\,\mathrm{K} \quad [16]\,. \tag{5}$$

At $T=813$ K the concentration of sodium atoms is $\mathrm{N_{Na}}(3s)=9.7.10^{16}\,\mathrm{cm}^{-3}$. Taking the limiting case of 50% population of the 3p level

$$\mathrm{N_{Na}}(3p)=\tfrac{1}{2}\mathrm{N_{Na}}(3s)=4.85\times10^{16}\,\mathrm{cm}^{-3}$$

we obtain, using the rate constants (3–5) the following characteristic time constants of the reactions (2)

$$\tau_{4\mathrm{d}}=4.1\ \mathrm{ms}\,, \tag{6}$$

$$\tau_{5\mathrm{s}}=2.9\ \mathrm{ms}\,, \tag{7}$$

$$\tau_{4\mathrm{p}}=68.7\ \mathrm{ms}\,. \tag{8}$$

From the other side, using the rate constants of Huennekens and Gallagher [17], the theoretical model as well as the experimental data of Müller et al. show that 5s–4p emission observed [18] by an energy-pooling mechanism is initiated several hundred nanoseconds after the start of the 1 µs pulse, pumping the red wing of Na–D line.

We conclude that although energy pooling, in principle, leads to population of 4p, the process is slow and in the time scale of the laser pulse the 4p population by this mechanism is negligible.

In spite of the fact that associative ionization has rate constants approximately 100 times greater compared to the rate constants of energy pooling [15], its contribution to the 4p population in time comparable or shorter than the laser pulse, is negligible.

Hence, the only mechanism, responsible for effective and fast population of 4p from 3p level is SERS. As shown by Lucatorto and McIlrath [19], the SERS mechanism at a pump intensity of $I=1\,\mathrm{MW}\times\mathrm{cm}^{-2}$ can transfer in 4p 15% of the population of 3p.

On the short-wavelength side of the excitation spectrum (Fig. 1b), for some of the lines, 4d is an intermediate state, enhancing the Raman process. For example, the detuning of the lines 5, 6, 7 and 8 (Fig. 1b) is −83.3, +26.4, +84.9, and +136.7 cm^{-1}, respectively. As seen from the figure, the intensity of the lines increases by decreasing the detuning from the 3p–4d resonance. At zero detuning the excitation intensity has a minimum due probably to multiphoton ionization.

The 4d level makes a considerable contribution to the SERS process on the broad maximum, marked as 4 in Fig. 1b, centered at 572 nm, with a detuning from the 3p–4d resonance of ~100 cm^{-1}. In the mechanism, proposed in [6], as an explanation for the 583 nm maximum, the authors considered 4p to be populated by two-photon absorption from dimer states and the

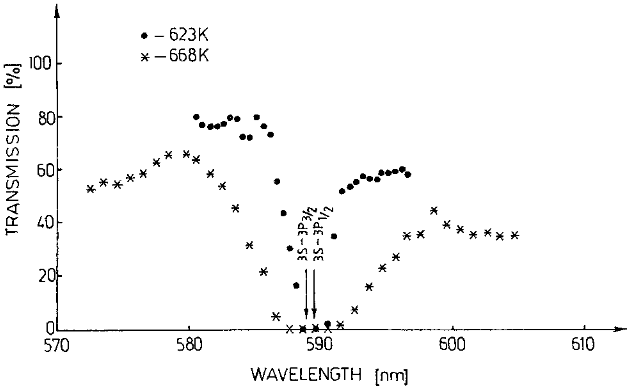

Fig. 3. Transmission of sodium recorded at two different temperatures

dissociation to $4p$. The strength of the molecular transition is 10 to 100 times smaller compared to the strong atomic resonance lines [20]. When a two-photon molecular transition has an intensity comparable to the $3s$–$4d$ resonance, an intermediate state with detuning $\leqq 1\ \mathrm{cm}^{-1}$ is supposed to enhance the first step, in our case $A\ {}^1\Sigma_u^+\ (v', J')$. Therefore, the population of $4p$ should not be a continuous function of wavelength, in spite of the fact that the second photon according to [6] is in the upper state continuum. Rather the measured excitation spectra would have maxima, reflecting approximately the $X-A$ vibrational-rotational structure contrary to the observed broad maxima. We conclude that the population of $4p$ in the vicinity of 583 nm is not caused by two-photon molecular absorption involving bound states and followed by direct dissociation in $4p$.

We have studied the absorption of the sodium heat pipe at $p_{\mathrm{Ar}} = 30$ Torr. The measured curves for two different temperatures are plotted in Fig. 3. As seen from the figure, there is a strong absorption around the single-photon resonance Na ($3s$–$3p$) even at considerable detuning. The width of the absorption dip is increased at higher sodium densities. A similar absorption was studied in Cs by Chen and Phelps [21].

The absorption observed is due to the Na – Ar as well as Na – Na colissional complexes when the sodium concentration $\mathrm{N_{Na}}$ is comparable to $\mathrm{N_{Ar}}$. The presence of strong absorption in the Na – D line wings and especially in the blue wing leads, after dissociation, to a considerable population of the Na ($3p$) level for large detuning of λ_d from the $3s$–$3p$ resonance.

The population of $3p$ is transfered to $4p$ by SERS. In fact, the real population of $4p$ by large detuning of λ_d in the blue wing of Na – D line was proved by Chen et al. [6], who observed orthogonal $4p$–$3s$ fluorescence.

The absorption in the blue wing of the Na – D line is in our view the origin of the broad maxima centered at 583 nm and 572 nm. Strong absorption in this spectral region can be predicted using the theoretical curves of Na – Ar of Saxon et al. [22] and $\mathrm{Na_2}$ of Konowalow et al. [23]. In the latter case, the curves were corrected for the actual value of the interval between the atomic asymptotes $3s$ and $3p$ [11]. The classical Franck-Condon principle was taken into account for the determination of the transition. According to it, the $X^2\Sigma - B^2\Sigma$ transition of Na–Ar collisional complex at the internuclear distance $R = 4.5 - 5.0$ Å is responsible for the absorption. Since the low lying levels of $\mathrm{Na_2}$ have seemingly not been investigated experimentally at large internuclear distances, we have used the theoretical curves of Konowalow et al. [23].

The absorption in the Na–Na collisional complex in the $X^1\Sigma_g^+ - B^1\Pi_u$ and $x^3\Sigma_u^+ - {}^3\Pi_g$ transitions at $R = 7 - 8$ Å also leads, after dissociation, to a population of $3p$ when the excitation wavelength λ_d is tuned to the blue wing of the Na–D line.

The transitions considered in Na–Ar and Na–Na are allowed by the molecular selection rules, which means that they have a large transition moment at the specified internuclear distances. The probability $S(v)$ for emission or absorption in the interval $v - v + dv$ is given by [24]

$$S(v)\,dv \sim \frac{n(R)\,4\pi R^2(v)\,dv}{|dv/dR|}, \tag{9}$$

where $n(R)$ is the density of the perturbing atom (Ar or Na) in the neighbourhood of the emitting atom (Na); $R(v)$ is the internuclear distance between Na and the perturbing atom at which the transition at frequency v takes place. For the respective $R(v)$ of the transitions $|dv/dR|$ for $B^2\Sigma$ (Na–Ar) is larger compared to $B^1\Pi_u$ and ${}^3\Pi_g$ (Na–Na). This, together with the fact that $R(v)$ for Na–Na is higher than $R(v)$ for Na–Ar collisions, means that, for densities $\mathrm{N_{Na}}$ comparable to $\mathrm{N_{Ar}}$, the Na–Na collisions might have a dominating role in the absorption in the range considered.

The $3p$ population has a maximum at λ_d tuned to the exact Na ($3s$–$3p$) resonance. However, in this case the whole energy of the pump beam is absorbed at the beginning of the vapor column and no energy is left for parametric or other additional processes. In this respect, the peak at 583 nm as well as the other peaks actually do not correspond to a maximum $3p$ population but to an optimum ratio between the power transfered to the atomic system and the power left for a parametric process and the $3p$–$4p$ SERS process.

By increasing the temperature T (and $\mathrm{N_{Na}}$) the maximum 2 is shifted to shorter wavelengths. Both 2 and 4 peaks have the same origin. However, the parametric maximum 4 arises from the closer vicinity to the $3p$–$4d$ resonance in spite of the larger detuning from $3s$–$3p$.

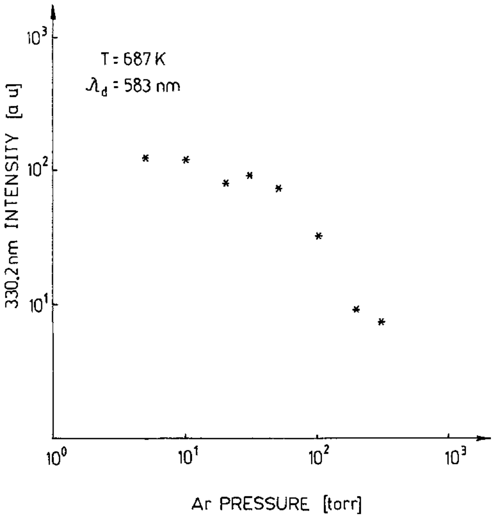

Fig. 4. Signal intensity as a function of Ar buffer gas pressure

We have measured the influence of P_{Ar} on the parametric process. As seen from Fig. 4, increasing P_{Ar} from 5 to 300 Torr the signal I_{330} intensity continuously decreases, which in our view, is caused by quenching of the parametric process by phase changing collisions.

The origin of excitation peaks, marked in Fig. 1b as 5, 6, 7, and 8 is, in our view, two-photon absorption from $X^1\Sigma_g^+$ to the bound part of high-lying molecular states followed by fast predissociation to $3p$. As discussed above, the strong two-photon transitions require intermediate rotational-vibrational levels of $A^1\Sigma_g^+$ detuned $\leq 1\,\mathrm{cm}^{-1}$. Together with Kroning's selection rules [25] this strongly reduces the number of possible transitions, leading to a population of $3p$ and explaines the small number of the peaks observed. Considering the symmetry of the intermediate A state, the upper level should be $^1\Sigma_g^+$ or $^1\Pi_g$. A strong predissociation follows when Kroning's selection rules and the Franck-Condon principle are fulfilled. According to the selection rules and the building-up principles these two photon populated states predissociates to $Na_2\,{}^1\Sigma_g^+(3s+3p)$ and $Na_2\,{}^1\Pi_g(3s+3p)$. Additional experimental data are needed to elucidate the exact mechanism of the descrete 5, 6, 7, and 8 lines.

Four-Wave Parametric Generation

Having populated the $4p$ state let us now consider the formation of the coherent parametric signal in the $4p$–$3s$ transition. The process does proceed through real population of the $4p$ level but it is not a laser transition. Inversion population to the ground state of sodium cannot be created. There are no metastable states, which could provide a reservoir, where the excited atoms accumulate while the pumping pulse continuously depopulate the ground state. Under such conditions, during a certain part of the pump pulse it would be possible to invert the population in some resonant transition as it is the case in Sr. Pumping resonantly the $5d\,{}^1D$ level of Sr Scheingraber and Vidal [26] observed lasing on resonant transitions, while three metastable states served as a drain for effective depopulation of the ground state.

In our case most of the atoms are in the ground state. We are not pumping directly an atomic transition but a molecular state, which, at the temperature used has the concentration of $N_{Na_2}/N_{Na} = 2$–3% [27].

Keeping the dye-laser wavelength fixed we have scanned the monochromator over the 330 nm region and recorded the wavelength and the form of the uv emission. The monochromator was callibrated using a Hg lamp in the visible and a Na lamp in uv. Shown in Fig. 5 is the emission spectrum recorded at the $\lambda_d = 598.66$ nm pumping wavelength. Also depicted is the position of the sodium resonant lines $4p_{3/2}$–$3s_{1/2}$ at 330.237 nm and $4p_{1/2}$–$3s_{1/2}$ at 330.298 nm of the spectral lamp. The doublet structure of the transition is clearly seen. However, both components are slightly shifted to the red side in this case. Tuning the pump wavelength through different resonances we measured the change in the spectral distribution between the doublet structure. The shift is an indication that the origin of the observed coherent emission is a parametric process and not lasing. In the latter case the lasing wavelength must coinside with the resonant transition because the lasing gain has a maximum on the line center. The parametric emission, on the other hand, does occur on the line wings due to the strong absorption on the line maximum, without inversion population.

We measured the forward-to-backward ratio of the emission. Within the experimental accuracy no signal in the backward direction was observed. This is another indication for the parametric origin of the emission. Lasing should occur in both directions, while

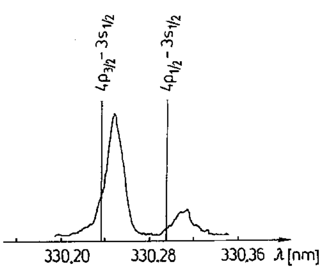

Fig. 5. Spectrum of the parametric emission taken at the excitation wavenumber $\nu_m = 16\,700.04\,\mathrm{cm}^{-1}$ (line No 15 in Table 1), pump power $P = 20$ kW, temperature $T = 687$ K and buffer gas pressure $p_{Ar} = 30$ Torr. The reference wavelengths are from a Na callibration lamp

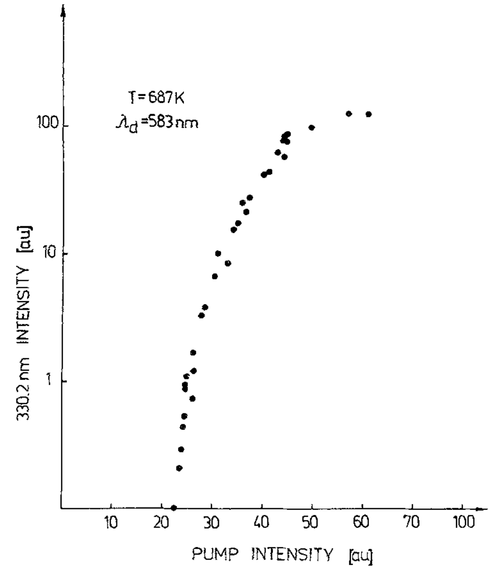

Fig. 6. UV signal *vs* dye-laser intensity

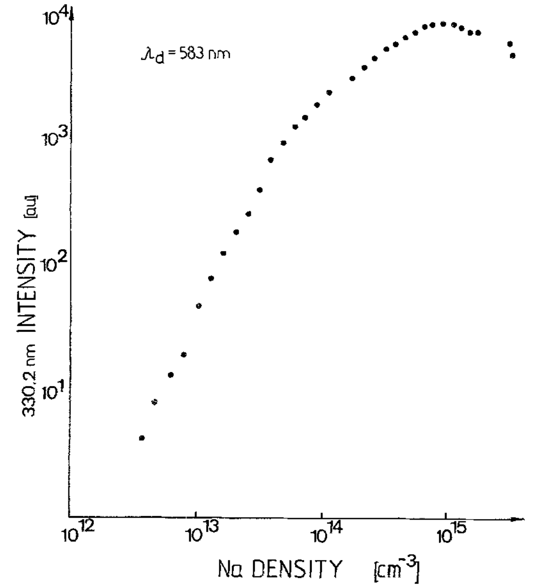

Fig. 7. 330 nm signal intensity as a function of sodium-vapor density

the signal wave ω_s of the four-wave parametric process is restricted by collinear index matching in the forward direction only.

The dependence of the 330 nm intensity on pump intensity was measured at several dye-laser wavelengths. Depicted in Fig. 6 are the results for $\lambda_d = 583$ nm, $N_{Na} = 7.2 \times 10^{15}\,cm^{-3}$ and $p_{Ar} = 30$ Torr. The dependence is exponential, characteristic for the signal wave in four-wave mixing [3].

Also in agreement with the theoretical prediction [3] is the dependence of the signal intensity on the sodium-vapor density, plotted in Fig. 7. In both cases saturation is observed due to strong multiphoton ionization and other limiting processes.

One can expect a deviation from the exact, fully parametric law due to the molecular contribution to the parametric process. A theoretical estimate for the parametric gain requires knowledge of the third-order nonlinear susceptibility $\chi^{(3)}$ and the detailed mechanism for pumping of $4p$ level.

Thus, our tentative explanation is that the coherent emission observed is a signal wave ω_s in the four-wave parametric generation

$$\omega_d + \omega_d = \omega_i + \omega_s\,. \tag{10}$$

The parametric process is connected with molecular absorption via real population of the $4p$ state. The resonant spontaneous emission from the radiative decay of $4p$ is amplified as a signal wave ω_s. In this way, ω_s starts not from noise but from a real, relatively strong spontaneous signal.

In principle, there are two other processes which can form the third wave in the four-wave mixing: optically pumped stimulated emission (OPSE) and stimulated electronic hyper Raman emission (SEHRS) [3]. In [6] OPSE $4d$–$4p$ and SERS emission at 2.34 μm were proposed as a third wave. The OPSE wavelengths, however, are fixed to the atomic transitions, thus the energy equation (1) can hold only at atomic resonance. The SERS, or more correctly SEHRS in this case, decreases continuously by detuning from the two-photon transition [1] and cannot account for the dip between the $4d$ resonance and the maximum at 583 nm in particular and for the complex structure in general. SEHRS cannot be excluded as a process giving rise as an initial wave ω_i in (1), but the influence of the molecules, leading to real population in Na and especially $4p$, is expressed in the contribution to the signal wave ω_s in (1) via $4p$–$3s$ spontaneous decay.

It is interesting to consider the problem of parametric generation in an excited-state medium. The parametric signal wave can stimulate the depopulation of $4p$ leading to its amplification. While $4p$ is not inverted, lasing is not possible. However, coupled with the parametric process slightly off exact resonance, the real population can enhance the stimulated process. More experimental data and theoretical work are needed to explain the detailed channels for absorption, energy transfer between molecules and atoms and the influence of the excited states on the nonlinear polarizabilities.

Conclusion

In conclusion, we have measured a number of narrow as well as broad resonances in the excitation spectra of the coherent resonant emission in sodium vapor. A mechanism is proposed including single and two-photon molecular absorption, transfer of real population to the 4*p* state of the atom and four-wave parametric generation enhanced through the radiative decay to the ground state.

Acknowledgements. One of us (S.G.D.) gratefully acknowledges research fellowship by the Alexander von Humboldt Stiftung and the Max-Planck-Gesellschaft zur Förderung der Wissenschaften. S.G.D. is especialy indebted to Prof. H. Walther for the constant help and to Dr. H.-U. Daniel for the valuable discussion and help in the experiment. The authors express their gratitude to Prof. K. Stamenov for the interest and support.

References

1. W. Hartig: Appl. Phys. **15**, 427 (1978)
2. J.R. Taylor: Opt. Commun. **18**, 504 (1976)
3. A.V. Smith, J.F. Ward: IEEE J. **QE-17**, 525 (1981)
4. P. Ewart, A.I.O'Leary: Opt. Commun. **40**, 147 (1981)
5. Y. Prior, A.R. Bogdan, M. Dagenais, N. Bloembergen: Phys. Rev. Lett. **46**, 111 (1981)
6. J.K. Chen, C.Y.R. Wu, C.C. Kim, D.L. Judge: Appl. Phys. B **33**, 155 (1984)
7. P. Kusch, M.M. Hessel: J. Chem. Phys. **68**, 2591 (1978)
8. M.E. Kaminsky: J. Chem. Phys. **66**, 4951 (1977)
9. W.T. Zemke, K.K. Verma, T. Vu, W.C. Stwalley: J. Mol. Spectrosc. **85**, 150 (1981)
10. K.K. Verma, J.T. Bahns, A.R. Rajaei-Rizi, W.C. Stwalley, W.T. Zemke: J. Chem. Phys. **78**, 3599 (1983)
11. S. Bashkin, J.O. Stoner, Jr.: *Atomic energy level and Grotrian diagrams*, Vol. 1 (North-Holland, Amsterdam 1975) p. 342
12. A.J. Taylor, K.M. Jones, A.L. Schawlow: Opt. Commun. **39**, 47 (1981)
13. P.P. Sorokin, J.R. Lankard: J. Chem. Phys. **54**, 2184 (1971)
14. M. Allegrini, G. Alzetta, A. Kopystynska, L. Moi, G. Orriols: Opt. Commun. **19**, 96 (1976)
15. V.S. Kushawaha, J.J. Leventhal: Phys. Rev. A **25**, 570 (1982)
16. V.S. Kushawaha, J.J. Leventhal: Phys. Rev. A **6**, 2468 (1980)
17. J. Huennekens, A. Gallagher: Abstract 8th ICAP Göteborg, 1982, ed. by I. Lindgren, A. Rosèn, S. Svanberg, A89 and references therein
18. W. Müller, J.J. McClelland, I.V. Hertel: Appl. Phys. B **31**, 131 (1983)
19. T.B. Lucatorto, T.J. McIlrath: Phys. Rev. Lett. **37**, 428 (1976)
20. G.P. Morgan, H.-R. Xia, A.L. Schawlow: J. Opt. Soc. Am. **72**, 315 (1982)
21. C.L. Chen, A.V. Phelps: Phys. Rev. **A7**, 470 (1973)
22. R.P. Saxon, R.E. Olson, B. Liu: J. Chem. Phys. **67**, 2692 (1977)
23. D.D. Konowalow, M.E. Rosenkrantz, M.L. Olson: J. Chem. Phys. **72**, 2612 (1980)
24. R.E.M. Hedges, D.L. Drummond, A. Gallagher: Phys. Rev. A **6**, 1519 (1972)
25. G. Herzberg: *Molecular Spectra and Molecular Structure I. Spectra of Diatomic Molecules*, 2nd ed. (Van Nostrand Reinhold, New York 1950)
26. H. Scheingraber, C.R. Vidal: IEEE J. **QE-19**, 1747 (1983)
27. M. Lapp, L.P. Harris: J. Quant. Spectrosc. Radiat. Transfer **6**, 169 (1966)